New Manzamine Alkaloids from an Indo-Pacific Sponge. Pharmacokinetics, Oral Availability, and the Significant Activity of Several Manzamines Against HIV-I, AIDS Opportunistic Infec...

ARTICLE *in* JOURNAL OF MEDICINAL CHEMISTRY · AUGUST 2004

Impact Factor: 5.45 · DOI: 10.1021/jm030475b · Source: PubMed

8 AUTHORS, INCLUDING:

Muhammad Yousaf
Riphah International University
67 PUBLICATIONS **485** CITATIONS
SEE PROFILE

Nicholas Hammond
University of Maryland Center for Environme...
7 PUBLICATIONS **139** CITATIONS
SEE PROFILE

Jiangnan Peng
University of North Carolina at Wilmington
67 PUBLICATIONS **1,369** CITATIONS
SEE PROFILE

Mark T Hamann
University of Mississippi
219 PUBLICATIONS **5,847** CITATIONS
SEE PROFILE

New Manzamine Alkaloids from an Indo-Pacific Sponge. Pharmacokinetics, Oral Availability, and the Significant Activity of Several Manzamines against HIV-I, AIDS Opportunistic Infections, and Inflammatory Diseases

Muhammad Yousaf,[†] Nicholas L. Hammond,[†] Jiangnan Peng,[†] Subagus Wahyuono,[‡] Kylie A. McIntosh,[§] William N. Charman,[§] Alejandro M. S. Mayer,[#] and Mark T. Hamann*,[†]

The Department of Pharmacognosy and National Center for the Development of Natural Products, School of Pharmacy, The University of Mississippi, University, Mississippi 38677, The Faculty of Pharmacy, Gadjah Mada University, Yogyakarta, Indonesia, Centre for Drug Candidate Optimisation, Victorian College of Pharmacy, Monash University (Parkville Campus), Parkville, Victoria 3052, Australia, and Department of Pharmacology, Chicago College of Osteopathic Medicine, Midwestern University, 555 31st Street, Downers Grove, Illinois 60515

Received September 22, 2003

12,28-Oxamanzamine A (**1**), 12,28-oxa-8-hydroxymanzamine A (**2**), and 31-keto-12,34-oxa-32,33-dihydroircinal A (**3**) were isolated from two collections of an Indo-Pacific sponge, and their structures were assigned on the basis of 1D and 2D NMR spectroscopic data. These compounds possess a novel manzamine-type ring system generated through a new ether bridge formed between carbons 12 and 28 or between carbons 12 and 34 of the typical manzamine structure and add to our growing understanding of manzamine SAR and metabolism. Based on molecular modeling studies, the formation of these oxidation products is highly sterically favored. The potent antiinflammatory, antifungal, and anti-HIV-1 activity for a number of previously reported manzamines is also presented in addition to the pharmacokinetic studies of manzamine A (**5**). Oral and intravenous pharmacokinetic studies of manzamine A in rats indicated the compound to have low metabolic clearance, a reasonably long pharmacokinetic half-life, and good absolute oral bioavailability of 20.6%, which supports the value of these compounds as potential leads for further preclinical assessment and possible development.

Introduction

As part of a continuing investigation of new manzamine-related alkaloids with activity against infectious and tropical disease,[1−5] three naturally occurring oxidation products including 12,28-oxamanzamine A (**1**), 12,28-oxa-8-hydroxymanzamine A (**2**), and 31-keto-12,34-oxa-32,33-dihydroircinal A (**3**) were isolated and characterized from an undescribed species of the genus *Acanthostrongylophora*. Each new manzamine contains an ether linkage unique to the structural class. Here, we describe the isolation, structure elucidation, and bioactivity of **1**−**3**. In addition, key oral and intravenous pharmacokinetic studies of manzamine A (**5**) have been completed and are reported here. Following exploratory dosing studies conducted in rats, the intravenous (iv) pharmacokinetic parameters of half-life, volume of distribution, and clearance could not be accurately determined from data obtained over an 8 h sampling period. To better define the iv and oral pharmacokinetic parameters of this promising drug lead, further dosing studies were conducted in rats employing an extended sampling period of 96 h.

Results and Discussion

The lipophilic extract of the freeze-dried sponge 01IND35 (4.5 kg) afforded, after repeated chromatography on silica gel, alumina and RP-HPLC, the new (+)-12,28-oxamanzamine A (**1**) (10.5 mg, 2.3×10^{-4} % dry wt), (+)-12,28-oxa-8-hydroxymanzamine A (**2**) (1.7 mg, 3.7×10^{-5} % dry wt), and a significant quantity of the antimalarial drug lead neokauluamine (3 g, 6.6×10^{-2} % dry wt).[2] The lipophilic extract of a second sample of the freeze-dried sponge 01IND35 collected on May 18, 2002, afforded the known (+)-manzamine A[6] (**5**) (10.5 g, 2.3×10^{-1} % dry wt), (+) manzamine F[7] (9.6 g, 2.1 ×

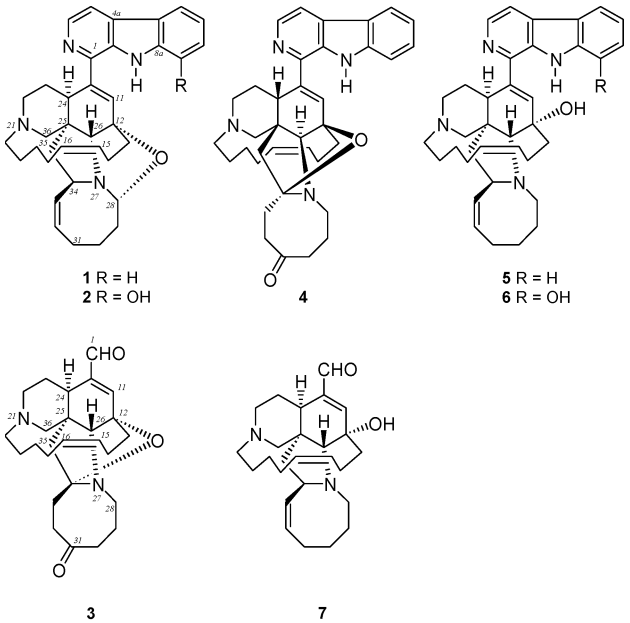

* To whom correspondence should be addressed. Telephone: 662-915-5730. Fax: 662-915-6975. E-mail: mthamann@olemiss.edu.
[†] The University of Mississippi.
[‡] Gadjah Mada University.
[§] Monash University.
[#] Midwestern University.

Table 1. ^{13}C and ^{1}H NMR Data of **1**−**3**[a]

	12,28-oxamanzamine A (**1**), δ		12,28-oxa-8-hydroxymanzamine A (**2**), δ		31-keto-12,34-oxa-32,33-dihydroircinal A (**3**), δ		ircinal A (**7**),[9] δ
position	^{13}C or ^{15}N	^{1}H	^{13}C	^{1}H	^{13}C or ^{15}N	^{1}H	^{13}C
1	142.9, s		143.7, s		193.9, d	9.47, s	193.3, d
N2	ND		ND				
3	138.8, d	8.46, d (5.1)	138.9, d	8.45, d (5.0)			
4	113.7, d	7.83, d (5.1)	114.3, d	7.83, d (5.0)			
4a	129.6, s		129.8, s				
4b	121.9, s		122.2, s				
5	121.6, d	8.10, d (7.8)	121.2, d	7.66, d (7.6)			
6	120.2, d	7.27, t (7.4)	120.5, d	7.14, t (7.4)			
7	128.4, d	7.53, t (7.1)	113.0, d	7.01, d (7.7)			
8	111.7, d	7.55, d (7.8)	143.4, s				
8a	141.4, s		136.3, s				
N9	ND	8.64, s	ND	9.18, s			
9a	133.6, s		133.7, s				
10	140.2, s		142.3, s		144.5, s		142.6, s
11	135.1, d	6.58, s	136.1, d	6.70, s	151.5, d	6.53, s	157.6, d
12	77.7, s		77.8, s		79.3, s		70.2, s
13	41.0, t	2.34, m	41.0, t	2.23, m	39.6, t	2.65, m	38.9, t
		1.63, m		2.01, m		2.32, m	
14	22.2, t	2.95, m	22.4, t	2.35, m	22.6, t	2.31, m	21.0, t
		2.35, m		1.95, m		2.41, m	
15	128.2, d	5.64, br s	138.3, d	5.60, br s	129.7, d	5.28, m	127.9, d
16	133.0, d	5.53, br s	133.7, d	5.53, br s	129.3, d	5.26, m	132.5, d
17	26.1, t	1.85, m	23.3, t	1.60, m	30.0, t	2.15, m	25.6, t
		1.78, m		1.54, m		2.23, m	
18	25.7, t	1.54, m	25.9, t	1.89, m	25.3, t	1.86, m	26.7, t
		1.34, m		1.55, m		1.73, m	
19	24.3, t	1.48, m	24.5, t	1.82, m	23.3, t	1.84, m	25.3, t
		1.40, m		1.72, m		1.69, m	
20	52.5, t	2.82, m	52.7, t	2.75, m	59.3, t	2.75, m	53.5, t
		2.37, m		2.32, m		2.44, m	
N21	ND		ND		38.3, S		
22	49.1, t	3.22, m	49.3, t	3.23, br d (9.3)	54.4, t	3.05, m	49.4, t
		2.14, m		2.25, m		2.15, m	
23	33.7, t	2.39, m	34.2, t	2.69, m	32.1, t	2.46, m	31.6, t
		2.64, m		2.15, m		2.31, m	
24	43.0, d	2.49, dd (11.8, 5.5)	43.4, d	2.63, dd (12.1, 5.2)	39.5, d	2.45, dd (12.0, 5.4)	34.0, d
25	42.5, s		42.3, s		37.7, s		46.4, s
26	76.0, d	4.35, s	76.0, d	4.37, s	68.0, d	4.24, s	76.3, d
N27	ND		ND		74.2, S		
28	94.7, d	4.69, t (8.3)	95.4, d	4.72, t (8.2)	49.8, t	3.37, dd (12.7, 11.6)	51.4, t
						2.83, dd (12.8, 4.6)	
29	26.7, t	1.75, m	26.4, t	1.54, m	30.0, t	1.83, m	29.8, t
		1.78, m		1.46, m		1.56, m	
30	26.9, t	1.62, m	26.9, t	1.95, 2H, m	31.4, t	1.69, m	25.3, t
		1.48, m				1.94, m	
31	23.3, t	3.25, m	27.0, s	3.32, m	201.2, s		28.2, t
		2.70, m		2.82, m			
32	132.8, d	5.37, m	133.1, t	5.37, m	30.8, t	2.85, m	137.1, d
						1.86, m	
33	123.9, d	5.35, m	124.1, t	5.31, m	29.9, t	2.85, m	127.7, d
						1.86, m	
34	60.9, d	3.75, d (7.2, 7.0)	61.3, s	3.79, dd (7.2, 7.1)	102.2, s		55.4, d
35	48.8, t	2.24, d (12.4)	49.0, t	2.32, d (12.4)	45.7, t	2.35, d (12.5)	44.6, t
		2.44, d (12.4)		2.26, d (12.4)		2.21, d (12.3)	
36	68.6, t	3.14, d (11.1)	68.8, t	3.18, d (11.1)	66.1, t	3.12, d (11.2)	69.2, t
		2.26, d (11.1)		2.32, d (11.1)		3.22, d (11.1)	

[a] In $CDCl_3$, 400 MHz for ^{1}H and 100 MHz for ^{13}C NMR and 50 MHz for ^{15}N NMR. Nitromethane was used as the external standard for ^{15}N NMR. Carbon multiplicities were determined by distortionless enhancement by polarization transfer (DEPT) experiments. s = quaternary, d = methine, t = methylene carbons. Coupling constants (J) are in Hz. NO = not observed. ND = not determined.

10^{-1} % dry wt), and the new (+)-31-keto-12,34-oxa-32,-33-dihydroircinal A (**3**) (16.8 mg, 3.7×10^{-4} % dry wt).

The high-resolution Fourier transform mass spectrum (HRFTMS) of **1** displayed a molecular ion peak (M + 1) at m/z 547.3414, which combined with ^{1}H and ^{13}C NMR data (Table 1) suggested a molecular formula of $C_{36}H_{42}N_4O$ and 18 degrees of unsaturation. A comparison of the data for this new compound with the literature data for (+)-12,34-oxamanzamine E (**4**)[1] indicated that compounds **1** and **4** had similar structures. The ^{13}C NMR signals in both compounds matched closely, while only C-28 and C-31 to C-34 differed substantially, indicating that these compounds have the same skeleton but have some differences in functionalities and oxygen substitution. The heteronuclear multiple-bond correlation (HMBC) spectra of both compounds showed similar correlations except for C-28 and C-34, confirming the same skeleton. The proton singlet resonating at δ 4.35 correlated to the nitrogenated methine carbon at δ 76.0 (C-26) in the heteronuclear multiple-

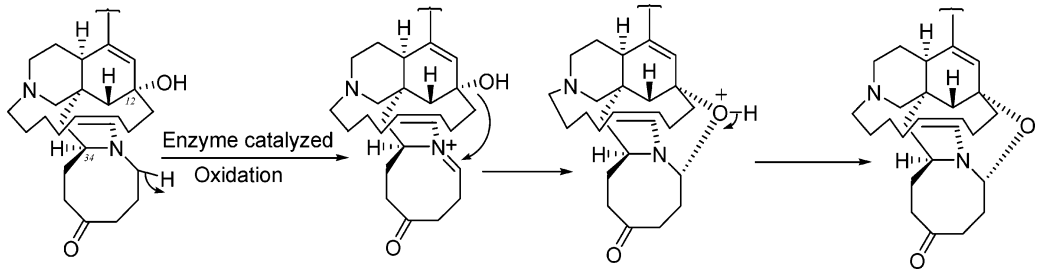

Figure 1. Plausible formation of 12,28-oxaether bridge via an oxidation mechanism.

quantum coherence (HMQC) spectrum and was assigned H-26. This proton showed HMBC correlations to a quaternary carbon (δ 77.7) and a methine carbon (δ 94.7), which were assigned as C-12 and C-28, respectively. The downfield shift of C-12 (δ 77.7) and C-28 (δ 94.7) in **1** compared with that of **4** suggested that the new ether bridge is between C-12 (C) and C-28 (CH) in **1** instead of between C-12 (C) and C-34 (C) as in **4**.[1] The lack of a keto group at C-31 and the presence of a double bond between C-32 and C-33 in **1** are clearly indicated by the compounds ^{1}H and ^{13}C NMR data.

^{1}H and ^{13}C NMR data of compound **2** revealed that it differed from **1** only in the carbocyclic ring of the β-carboline moiety (C-5 to C-8a, Table 1). An additional oxygen atom in the molecular formula of **2** ($C_{36}H_{42}N_4O_2$) suggested a phenolic hydroxyl, which is also shown by the ^{1}H NMR spectrum exhibiting five aromatic proton signals instead of six, combined with a new downfield oxygenated aromatic quaternary carbon at δ 143.4 (C-8) in **2**. The relative stereochemistry of **1** and **2** was deduced from the nuclear Overhauser effect spectrometry (NOESY), which showed NOE correlations between H-26 and H-28 as well as between H-24 and H-35. The 12,28-oxaether bridge was assigned α-orientation based on retention of stereochemistry of the C-12 oxygen in the parent compounds manzamine A[6] (**5**) and 8-hydroxymanzamine A[8] (**6**) during the formation of the ether bridge through a proposed enzymatic oxidation followed by intramolecular quenching of the cation by the 12-OH group (Figure 1). The absolute and relative stereochemistry of **1** and **2** would then be analogous to that of **5** and **6** and is further supported by NOE data (NOE correlations between H-26 and H-28 as well as between H-24 and H-35), optical rotation values, and molecular modeling ($[\alpha]_D^{25}$ +38 for **1** and +8 for **2** in $CHCl_3$).[6,8]

The lipophilic extract (3.5 kg) of the sponge 01IND35 (second collection) afforded compound **3**. The ^{1}H and ^{13}C NMR data of compound **3** exhibited a close resemblance to that of ircinal A (**7**)[9] (Table 1). The HRFTMS of **3** suggested the molecular formula $C_{26}H_{36}N_2O_3$ and indicated the presence of one more double bond equivalent compared with that of ircinal A (**7**).[9] This suggested the presence of a new ether bridge between C-12 and C-34, similar to that of **4**, which was confirmed by ^{13}C NMR data. The downfield quaternary carbon signal at δ 201.2 was assigned as the C-31 ketone group, based on its HMBC correlations with H_2-29 and H_2-33. Other key HMBC correlations were observed between H-1 and C-10, between C-11 and C-24, and between H-26 and C-12 and C-34 supporting the structure of compound **3**. The relative stereochemistry was determined to be analogous to that of ircinal A (**7**),[9] based on NOESY, which showed NOE correlations between H-24 and H-35. In addition, the retention of stereochemistry of the C-12 oxygen in the parent compound **7** during the formation of the ether bridge is supported by the optical rotation value of $[\alpha]_D^{25}$ +44 in $CHCl_3$ combined with molecular modeling.

The highly promising antituberculosis and antimalarial activities of the manzamines have been reported previously.[1−5] The common manzamines were assayed for antiinflammatory, antibacterial, antifungal, and antihuman immunodeficiency virus (HIV-1) activity, and these additional data against infectious diseases are reported here (Table 2). Manzamine A, 8-hydroxymanzamine A, 6-deoxymanzamine X, and neokaulumine were active against *Staphylococcus aureus*, methicillin-resistant *S. aureus*, *Cryptococcus neoformans*, and *Mycobacterium intracellulare*, having MIC values in the range 0.5−6.25 μg/mL. Manzamine A, 8-hydroxymanzamine A, 6-deoxymanzamine X, and neokauluamine showed significant anti-HIV-1 activity with EC_{50} of 4.2, 0.59, 1.6, and 2.3 μM, respectively. The absence of activity for **1**−**3**, 12,34-oxamanzamine E and F, and manzamine E and F is clearly associated with the presence of a C-31 ketone group, reduction of the double bond, or the formation of the ether bridge between carbons 12 and 28 or between carbons 12 and 34. The antiinflammatory activity of ent-8-hydroxymanzamine A and neokauluamine was determined as previously described[10] by investigating the effect of these compounds on the release of rat neonatal brain microglia superoxide anion and thromboxane B_2, mediators thought to be involved in neuroinflammatory conditions[11] and lactate dehydrogenase (LDH), a marker for cell toxicity.[12] Both ent-8-hydroxymanzamine A and neokauluamine were relatively ineffective inhibitors of both phorbol ester stimulated thromboxane B_2 (IC_{50} > 30 μM) and superoxide anion (IC_{50} > 30 μM) generation as well as rather nontoxic to the microglia cells in vitro (LDH_{50} > 30 μM).

The plasma concentration versus time profiles for manzamine A are presented in Figure 2, with concentrations remaining well above the assay limit of quantitation (LOQ) (10 ng/mL) throughout the entire 96 h sampling period following both iv and oral administration. After iv administration of manzamine A to rats at a dose of 10 mg/kg, the half-life, apparent volume of distribution, and plasma clearance were estimated from the mean plasma concentration data (from $n = 3$) to be 53.7 h, 23.7 L/kg, and 5.1 (mL/min)/kg, respectively. As noted in the earlier dosing studies, urine collected from these animals was red for approximately 2 h following the iv administration of manzamine A. After this time, however, it was observed that the color of the urine

Table 2. Bioactivity Data for Manzamines[a]

compd	assay: antibacterial IC_{50} (μg/mL): *Staphylococcus aureus*	assay: antibacterial IC_{50} (μg/mL): methicillin-resistant *Staphylococcus aureus*	assay: antifungal IC_{50} (μg/mL): *Cryptococcus neoformans*	assay: antifungal IC_{50} (μg/mL): *Mycobacterium intracellulare*	assay: HIV EC_{50} (μM)
12,28-oxamanamine A (**1**)	NA	NA	NA	NA	22.2
12,28-oxa-8-hydroxymanzamine A (**2**)	NA	NA	NA	NA	NT
31-keto-12,34-oxa-32,33-dihydroircinal A (**3**)	NA	NA	NA	NA	NT
12,34-oxamanzamine E	NA	NA	NA	NA	17.5
12,34-oxamanzamine F	NA	NA	NA	NA	14.9
neokauluamine	NA	NA	3.0	3.0	2.3
manzamine A (**5**)	0.5	0.7	3.0	0.35	4.2
8-hydroxymanzamine A (**6**)	0.9	4.0	3.0	1.0	0.59
6-deoxymanzamine X	1.5	1.5	2.0	6.25	1.6
manzamine E	NA	NA	NA	12.5	13.1
manzamine F	NA	NA	6.5	6.25	7.3
ircinal A	NA	NA	NA	NA	6.8
ircinol A	NA	30	NA	50	4.3
amphotericin B	NT	NT	0.15	NT	NT
ciprofloxacin	0.10	0.10	NT	0.25	NT
AZT[13]	NT	NT	NT	NT	0.004

[a] NA = not active. NT = not tested.

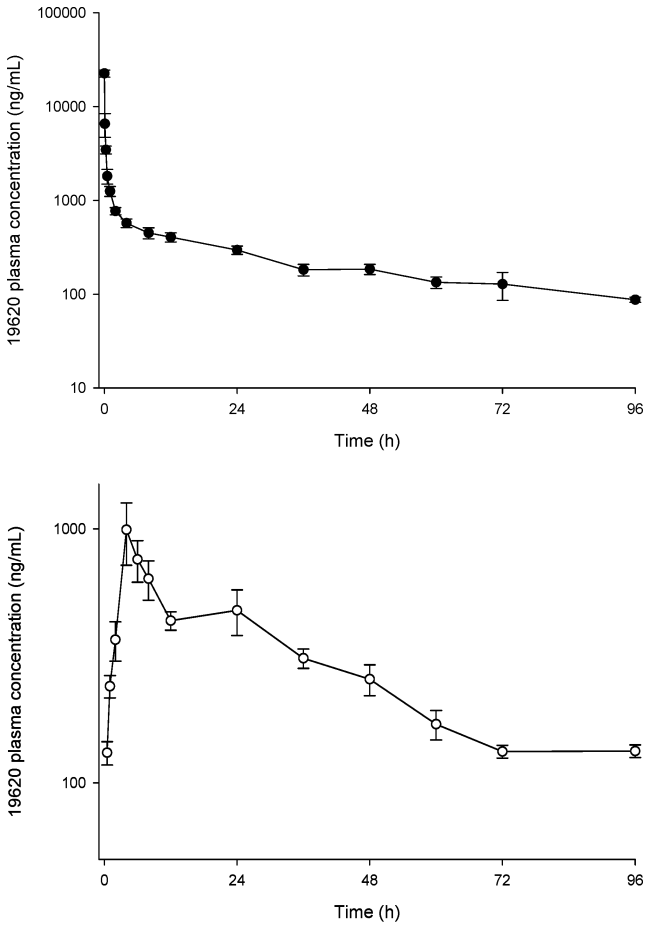

Figure 2. Average plasma concentration versus time profiles for TDR 19620 after iv (top) and oral (bottom) administration to rats at a dose of approximately 10 and 50 mg/kg, respectively (±SEM for $n = 3-4$). The LOQ of the HPLC/MS assay for TDR 19620 was 10 ng/mL.

returned to a normal clear-yellow color. Collected plasma samples also showed evidence of hemolysis, and no evidence of discoloration in urine or plasma samples was noted in a control animal dosed intravenously with a drug-free iv formulation, indicating that these effects were unlikely due primarily to the vehicle.

After oral administration to rats at a dose of 50 mg/kg, the absolute oral bioavailability of manzamine A was approximated using truncated area under the curve (AUC) values for the oral and iv profiles (AUC_{0-96}), resulting in an absolute oral bioavailability of 20.6 ± 1.3% (mean ± SEM for four rats). It is probable that while this estimate is still somewhat lower than the "actual" value because of the need to use truncated AUC values, it nevertheless indicates reasonable oral bioavailability in rats after administration in an aqueous suspension. The C_{max} and T_{max} values were 1066 ± 177 ng/mL and 10 ± 5 h, respectively. This report describes the first published pharmacokinetic studies of manzamine A. Most importantly, the oral bioavailability of manzamine A in rats was estimated to be at least 20.6%. Furthermore, plasma concentrations were observed to remain well above the assay LOQ in all animals for the duration of the 96 h study.

The sampling period employed in the current study enabled the estimation of the iv pharmacokinetic parameters of manzamine A, which demonstrated a very long half-life and low plasma clearance. The in vitro metabolism studies of manzamine A conducted previously in human liver microsomes support the likelihood of slow hepatic metabolism, predicting a low hepatic extraction ratio of 0.4.

The basis for the good oral bioavailability of manzamine A is likely to result from reasonable metabolic stability and good absorption. The acid solubility of manzamine A suggests that the compound should readily dissolve in the stomach, while the compound is expected to be reasonably permeable in light of its high log *P* (8.34) that was determined using a chromatographic method.

This study has provided the first published information regarding the pharmacokinetic properties of manzamine A in rats. It is likely that the very long half-life and low plasma clearance of this interesting compound may have significant pharmacodynamic implications with respect to its reported excellent antimalarial activity.

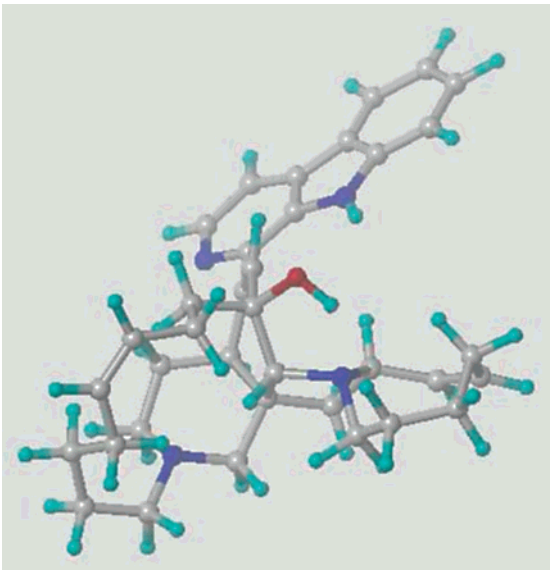

Figure 3. Minimized energy conformation of manzamine A

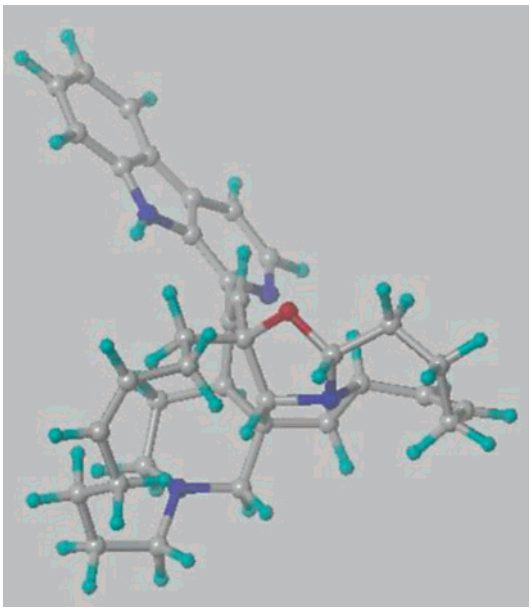

Figure 4. Minimized energy conformation of 12,28-oxamanzamine A (1).

Molecular Modeling

Manzamine A exhibited significant antibacterial, antifungal, and anti-HIV activity, while 12,28-oxamanzamine A, the oxidative cyclization product of manzamine A, did not show notable biological activity. To better understand the structure−activity relationship and possible steric affects contributing to this oxidation, a molecular modeling study was performed using a Sybyl 6.8 software package. The minimized energy conformations of manzamine A and 12,28-oxamanzamine A are shown in Figures 3 and 4, respectively. The minimized energy conformation of manzamine A is highly comparable to the conformation of crystalline manzamine A hydrochloride[6] determined by X-ray diffraction with the exception of the $C_{25}-C_{26}-N_{27}-C_{34}-C_{35}$ five-membered ring and the $N_{27}-C_{34}$ eight-membered ring. On the basis of the crystal structure of manzamine A hydrochloride, the difference between the solution-phase structure and X-ray structure clearly arose from the ionic bond between N_{27} and the chloride ion. The minimized energy conformation of 12,28-oxamanzamine A is very close to that of manzamine A with minor differences appearing at the $N_{27}-C_{34}$ eight-membered ring. The $N_{27}-C_{34}$ eight-membered ring is folded upward in 12,28-oxamanzamine A and the configuration of the N-27 is enantiomeric, suggesting that the antimicrobial and anti-HIV activity may be closely related to N-27 and the conformation of the $N_{27}-C_{34}$ eight-membered ring.

Experimental Section

General Experimental Procedures. The ^{1}H and ^{13}C NMR spectra were recorded in $CDCl_3$ on a Bruker DRX NMR spectrometer operating at 400 MHz for ^{1}H and at 100 MHz for ^{13}C NMR. Chemical shift (δ) values are expressed in parts per million (ppm) and are referenced to the residual solvent signals of $CDCl_3$ at δ_H/δ_C 7.26/77.0. The HRMS data were measured on a Bioapex FTMS with electrospray ionization. The IR spectra were recorded on an ATI Mattson Genesis series FTIR spectrophotometer. UV spectra were scanned on a Perkin-Elmer Lambda 3B UV/vis spectrometer. Silica gel (200−400 mesh) and alumina (63−200 μm) were obtained from Natland International Corporation (www.natland.com) and Scientific Adsorbents Incorporated (www.saisorb.com), respectively. TLC was performed on aluminum sheets (silica gel 60 F_{254}, Merck KGaA, Germany).

Sponge Collection, Identification, and Taxonomy. Sponge collection, identification, taxonomy, and extraction for 01IND35 have been described elsewhere.[1] The sponge was collected for the second time from reef slopes and vertical surfaces between 6 and 33 m from Black Reef Point, Manado Bay, Indonesia, on May 18, 2002, by Professor Subagus Wahyuono and his research group.

(+)-12,28-Oxamanzamine A (1): amorphous solid ($CHCl_3$); mp 148 °C dec, $[\alpha]_D^{25}$ +38 (*c* 0.1, $CHCl_3$); UV λ_{max} (log ϵ) (MeOH) 253 (3.81), 274 (3.66), 352 (3.41) nm; IR ν_{max} ($CHCl_3$) 3650 (NH), 3001−2818, 1620, 1592, 1533, 1452, 1267, 1144, 1052 cm^{-1}; HRFABMS *m*/*z* calcd for $C_{36}H_{43}N_4O$ $(M + H)^+$ 547.3386, found 547.3414. For ^{1}H and ^{13}C NMR, see Table 1.

(+)-12,28-Oxa-8-hydroxymanzamine A (2): amorphous powder (EtOH); mp 160 °C dec; $[\alpha]_D^{25}$ +8 (*c* 0.10, $CHCl_3$); UV λ_{max} (log ϵ) (MeOH) 251 (3.85), 273 (3.78), 356 (3.38) nm; IR ν_{max} ($CHCl_3$) 3658 (NH), 3377 (OH), 3002−2822, 1620, 1592, 1533, 1452, 1267, 1144, 1052 cm^{-1}; HRFABMS *m*/*z* calcd for $C_{36}H_{43}N_4O_2$ $(M + H)^+$ 563.3335, found 563.3313. For ^{1}H and ^{13}C NMR, see Table 1.

(+)-31-Keto-12,34-oxa-32,33-dihydroircinal A (3): white powder (MeOH); mp 164 °C (dec); $[\alpha]_D^{25}$ +44 (*c* 0.1, $CHCl_3$); UV λ_{max} (log ϵ) (MeOH) 235 (3.929) nm; IR ν_{max} ($CHCl_3$) 3368 (OH), 3001−2815, 1695 (C=O), 1625, 1590, 1535, 1451, 1265, 1145, 1050 cm^{-1}; HRFABMS *m*/*z* calcd for $C_{26}H_{37}N_2O_3$ $(M + H)^+$ 425.3408, found 425.3458. For ^{1}H and ^{13}C NMR, see Table 1.

Pharmacokinetic Studies. Pharmacokinetic studies were conducted in male Sprague-Dawley rats and included individual iv and oral administration of manzamine A. Briefly, on the day prior to dosing, rats (280−320 g) had polyethylene cannulae surgically implanted in the right jugular vein and/or left carotid artery. Animals were fasted but had free access to water until 12 h following dosing, after which free access to food was also resumed.

Intravenous formulations were prepared at an approximate concentration of **3** mg/mL manzamine A in 10% v/v ethanol in 50 mM tartrate buffer, pH 3.0, to enable a nominal iv dose of 10 mg/kg with a 1 mL dosing volume. The oral formulation was prepared using a standard aqueous suspending vehicle (SSV, 0.5% CMC, 0.5% benzyl alcohol, 0.4% Tween-80 in 0.9% NaCl) to provide a nominal dose of 50 mg/kg. Intravenous doses were administered as a 5 min infusion via the jugular vein cannula, and oral doses were administered by gavage.

Blood samples were withdrawn from an in-dwelling carotid cannula over a 96 h period. Samples were stored on ice until centrifugation to separate plasma from red blood cells, and a 100 mL aliquot of plasma was transferred to a fresh Eppendorf tube and stored at −20 °C until analysis. A validated HPLC/MS method was developed and employed for determination of manzamine A plasma concentrations, and Winnonlin software (version 1.5, Scientific Consulting, Inc.) was utilized for pharmacokinetic parameter estimation.

Molecular Modeling. The molecular modeling studies were performed on a Silicon Graphics Octane2 workstation. The molecular structure was constructed using standard geometries and standard bond lengths in the Sybyl 6.8 software package and was manipulated using the standard Tripos force. The initial conformations of the molecule were obtained from 10 rounds of simulated annealing experiments. In each round of simulation, the molecule was heated to 500 K within 500 fs and then allowed to cool to 200 K within 5000 fs. Ten energy optimal conformations were selected and refined by minimization using Powell's method, MMFF94 force field, and partial charges until a root-mean-square deviation of 0.001 kcal/(mol·Å) was achieved. A distance-dependent dielectric of 1.00 was used throughout the calculation. A strategy of simplex algorithm followed by conjugate gradient algorithm was used in the minimization. Finally, from these refined conformations, the conformer with the lowest energy was selected as the final molecular conformation.

Acknowledgment. John Trott and Sharon Sanders are gratefully acknowledged for in vitro antibacterial and antifungal assays. We are grateful to Professor Raymond Schinazi's program for performing anti-HIV-1 evaluation and to Frank Wiggers and Chuck Dunbar for ^{15}N NMR and mass spectral data. Dr. Waseem Gul and Ms. Marwa Donia are thanked for helpful discussions. This work was supported by Public Health Service Grant 1 R01 AI 36596 from the National Institute of Allergy and Infectious Diseases, The Medicines for Malaria Venture and The Center for Disease Control. Funding for the antiinflammatory studies was provided by Midwestern University (to A.M.S.M.).

References

(1) Yousaf, M.; El Sayed, K. A.; Rao, K. V.; Lim, C. W.; Hu, J. F.; Kelly, M.; Franzblau, S. G.; Zhang, F.; Olivier, P.; Hill, R. T.; Hamann, M. T. 12,34-Oxamanzamines, novel biocatalytic and natural products from manzamine producing Indo-Pacific sponges. *Tetrahedron* **2002**, *58*, 7397−7402.

(2) El Sayed, K. A.; Kelly, M.; Kara, U. A. K.; Ang, K. K. H.; Katsuyama, I.; Dunbar, D. C.; Khan, A. A.; Hamann, M. T. New manzamine alkaloids with potent activity against infectious diseases. *J. Am. Chem. Soc.* **2001**, *123*, 1804−1808.

(3) Ang, K. K. H.; Holmes, M. J.; Higa, T.; Hamann, M. T.; Kara, U. A. K. In vivo antimalarial activity of the *β*-carboline alkaloid manzamine A. *Antimicrob. Agents Chemother.* **2000**, *44* (6), 1645−1649.

(4) Rao, K. V.; Santarsiero, B. D.; Mesecar, A. D.; Schinazi, R. F.; Tekwani, B. L.; Hamann, M. T. New manzamine alkaloids with activity against infectious and tropical parasitic diseases from an Indonesian sponge. *J. Nat. Prod.* **2003**, *66*, 823−828.

(5) Hu, J. F.; Hamann, M. T.; Hill, R. T.; Kelly, M. The Manzamine Alkaloids. In *The Alkaloids: Biology and Chemistry*; Cordell, G. A., Ed.; Elsevier: Oxford, U.K., 2003; Vol. 60, pp 207−285.

(6) Sakai, R.; Higa, T.; Jefford, C. W.; Bernardinelli, G. Manzamine A, a novel antitumor alkaloid from a sponge. *J. Am. Chem. Soc.* **1986**, *108*, 6404−6405.

(7) Ichiba, T.; Sakai, R.; Kohmoto, S.; Saucy, G.; Higa, T. New manzamine alkaloids from a sponge of the genus Xestospongia. *Tetrahedron Lett.* **1988**, *29* (25), 3083−3086.

(8) Ichiba, T.; Corgiat, J. M.; Scheuer, P. J.; Borges, M. K. 8-Hydroxymanzamine A, a *β*-carboline alkaloid from a sponge, Pachypellina sp. *J. Nat. Prod.* **1994**, *57*, 168−170.

(9) Kondo, K.; Shigemori, H.; Kikuchi, Y.; Ishibashi, M.; Sasaki, T.; Kobayashi, J. Ircinals A and B from the Okinawan marine sponge Ircinia sp.: plausible biogenetic precursors of manzamine alkaloids. *J. Org. Chem.* **1992**, *57*, 2480−2483.

(10) El Sayed, K. A.; Mayer, A. M. S.; Kelly, M.; Hamann, M. T. The Biocatalytic Transformation of Furan to Amide in the Bioactive Marine Natural Product Palinurin. *J. Org. Chem.* **1999**, *64*, 9258−9260.

(11) Mayer, A. M. Therapeutic implications of microglia activation by lipopolysaccharide and reactive oxygen species generation in septic shock and central nervous system pathologies: a review. *Medicina (Buenos Aires)* **1998**, *58*, 377−385.

(12) Mayer, A. M. S.; Oh, S.; Ramsey, K. H.; Jacobson, P. B.; Glaser, K. B.; Romanic, A. M. *Escherichia coli* lipopolysaccharide potentiation and inhibition of rat neonatal microglia superoxide anion generation: correlation with prior lactic dehydrogenase, nitric oxide, tumor necrosis factor-α, thromboxane B_2 and metalloprotease release. *SHOCK* **1999**, *11*, 180−186.

(13) Schinazi, R. F.; McMillan, A.; Cannon, D.; Mathis, R.; Lloyd, R. M.; Peck, A.; Sommadossi, J.-P.; St. Clair, M.; Wilson, J.; Furman, P. A.; Painter, G.; Choi, W.-B.; Liotta, D. C. Selective Inhibition of Human Immunodeficiency Viruses by Racemates and Enantiomers of *cis*-5-Fluoro-1-[2-(hydroxymethyl)-1,3-oxathiolan-5-yl] Cytosine *Antimicrob. Agents Chemother.* **1992**, *36*, 2423−2431.